Fixed-height exit bender of synchrotron X-rays above 40 keV

Yasuhiro Yoneda,[a]* Norimasa Matsumoto,[a] Yukito Furukawa[b] and Tetsuya Ishikawa[b,c]

[a]Japan Atomic Energy Research Institute (JAERI), 1-1-1 Kouto, Mikazuki-cho, Sayo-gun, Hyogo 679-5148, Japan, [b]Japan Synchrotron Radiation Research Institute (JASRI), 1-1-1 Kouto, Mikazuki-cho, Sayo-gun, Hyogo 679-5198, Japan, and [c]Institute of Physical and Chemical Research (RIKEN), 1-1-1 Kouto, Mikazuki-cho, Sayo-gun, Hyogo 679-5148, Japan. E-mail: yoneda@spring8.or.jp

A crystal bender for sagittal focusing has been designed for standard monochromators at SPring-8. The bender does not move the position of the crystal center when the bending radius is changed. Sagittal focusing from 40 keV to 60 keV was achieved by using Si(311) double crystals. The flux density of the focused beam measured at 40 keV was 15 times higher than that of the unfocused beam. The height deviation of the focused beam throughout the measured energy range was within ± 0.15 mm.

Keywords: fixed-height exit benders; bent crystals; high-energy synchrotron radiation.

1. Introduction

Sagittal focusing (*e.g.* Sparks *et al.*, 1980, 1982) is known as one of the most efficient focusing methods for synchrotron X-rays which increases the photon density at the sample position. Usually the second crystal of a double-crystal monochromator is bent in a cylindrical shape, ideally without introducing any deformation of the crystal in the scattering plane. Accordingly, both energy and momentum resolutions are kept as high as those for flat–flat double-crystal monochromators. The bent radius for the optimal focus is a function of the Bragg angle – the radius becomes smaller as the Bragg angle decreases. Various bending mechanisms for sagittal focusing have been developed (Pascarelli *et al.*, 1996; Matsushita *et al.*, 1986; Koyama *et al.*, 1991). However, most applications have been restricted to relatively low-energy X-rays owing to the difficulty of ideally bending crystals of small radii. In addition, the simultaneous fulfillment of optimal focus and fixed exit in changing output energy is preferable for most applications. This may add some complexity to the bending mechanism.

This paper reports the results of both high-energy sagittal focusing and fixed-exit focusing using an Si(311) double-crystal monochromator. A reasonably good focusing was achieved at 40 keV. The height variation of the focus points from 40 keV to 60 keV remained within 0.3 mm when the bent radius was optimized according to respective energy values.

2. Description of the monochromator crystal and bender

Although rhombohedral or double-triangle ribbed crystals bent with a cam driver mechanism (Matsushita *et al.*, 1986) provide a fixed-exit condition, they are apt to introducing a non-uniform bend owing to the cramp at the crystal center. We have developed a new sagittal-focus bender (Furukawa & Ishikawa, 1995) that is compatible with the SPring-8 standard monochromator (Uruga *et al.*, 1995; Yabashi *et al.*, 1999) for bending-magnet beamlines. The bender uses, in principle, the conventional four-point bending mechanism, but the rollers for four-point bending are attached to rotation arms so as to make the center position of the crystal being fixed irrespective of the bending radius. This is based on a simple geometrical theorem illustrated in Fig. 1(*a*). Two circles *A* and *B* in Fig. 1 are always across at the right angles to the circles *C* and *D*, the centers O_C and O_D of which are on the perpendicular bisector *L* of the centers of circles *A* and *B*. This shows that the crystal, which corresponds to the circle *C* or *D* in Fig. 1, is bent cylindrically without changing the height of the middle point

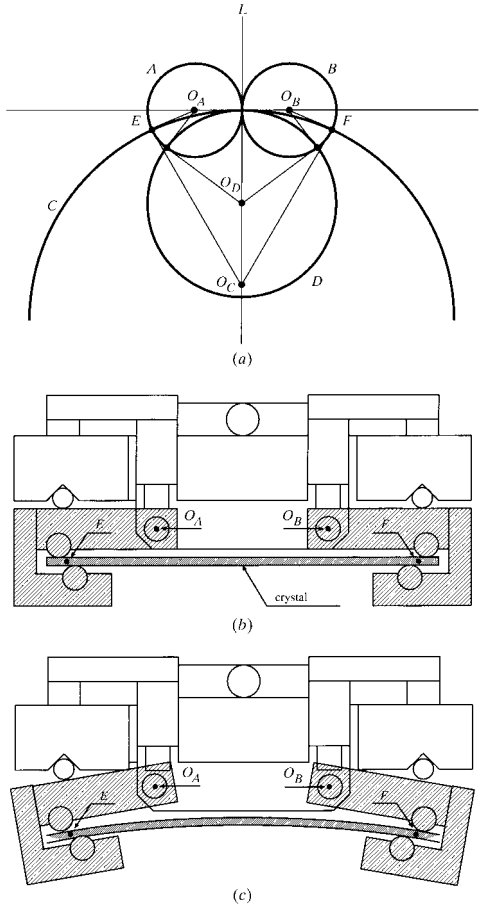

Figure 1
(*a*) Geometrical condition of the fixed-exit bender. (*b*) Actual bending mechanism when the crystal is flattened and (*c*) when the crystal is bent.

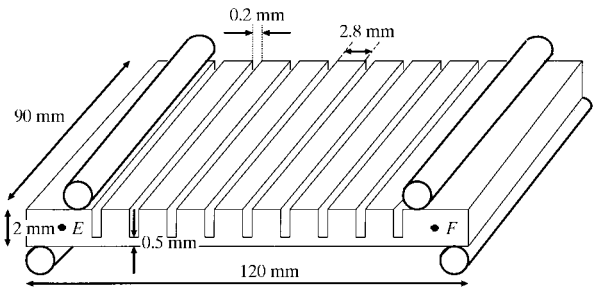

Figure 2
Schematic diagram of a series of crystal slabs joined by thin hinges, cut parallel to the bending rods.

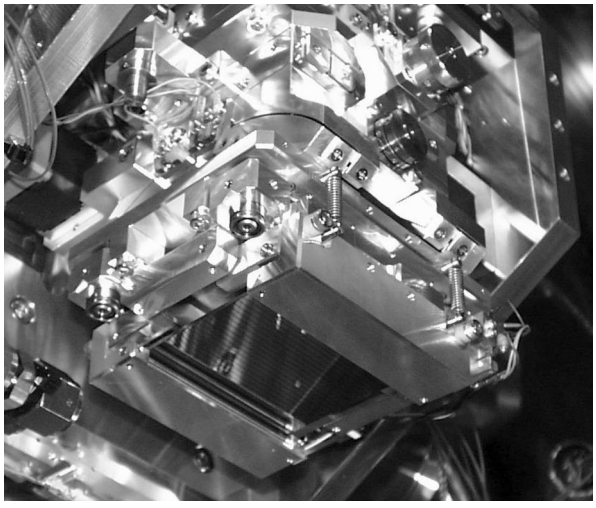

Figure 3
Sagittal-focus bender for a series of crystal slabs joined by thin hinges installed in the standard monochromator as the second crystal.

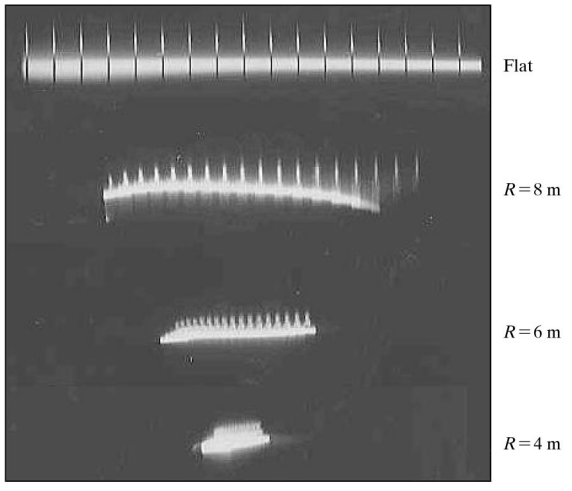

Figure 4
Beam profiles with the sagittally focusing crystal monochromator at 40 keV. The period of the slotted crystal is 3 mm. The X-ray beam was focused as the bending radius R decreased.

of the arc of the circle C or D, when pure torque is applied at the cross points E and F. The actual bending mechanism when the crystal is flattened is shown in Fig. 1(b). The crystal was cramped with four cylindrical rollers of the cradle [grey part in Figs. 1(b) and 1(c)]. The bending is performed by rotating the cradle around O_A and O_C, so that the crystal is bent without changing the center position as shown in Fig. 1(c).

Since the SPring-8 standard monochromator is designed to fix the exit-beam height in changing energy, a combination of the bending mechanism with the monochromator also fixes the exit-beam height with optimized bending radius for each energy.

We used a series of crystal slabs joined by thin hinges. Each slab is made of an Si(311) plate with a rectangular shape of 90 mm (along the beam) × 100 mm (across the beam) × 2 mm (thickness) as shown in Fig. 2, in order to avoid anti-classical bending (Kushnir *et al.*, 1993, 1995) that degrades the total throughput.

3. Experimental results

The focusing test was carried out at beamline 14B1 of SPring-8, which is a bending-magnet beamline dedicated to JAERI equipped with a SPring-8 standard double-crystal monochromator. The fixed-exit bender was mounted on the second crystal stage of the monochromator as shown in Fig. 3. A pair of Si(311) crystals were used both for the first and second crystals. For the first crystal, an indirectly cooled flat plate was used instead of the standard SPring-8 direct fin-cooled crystal. The electron beam current during the test was ∼70 mA.

The horizontal divergence of the incident beam to the monochromator was defined by a water-cooled four-jaw slit (40 mm width × 5 mm height) upstream of the monochromator. The monochromator was located at 36.5 m (F_1 = 36.5 m) from the source, where the horizontal beam size of the beam on the first crystal was 50 mm. Focus observation was performed using a TV camera recording an image on a ZnS fluorescent screen placed at a point 48.5 m from the source, so that the monochromator–focus point distance, F_2, was 16.5 m. These distances give magnifications ($M = F_2/F_1$) of approximately 1/3.

Fig. 4 shows the observed beam profiles at 40 keV with different bending radii R. The horizontal beam size was 65 mm at the screen position for the unbent crystal. The beam reflected from the slot part of the crystal appeared like teeth of a comb. We can appreciate the number of slots reflecting the X-ray beam by counting the sharp lines. From the image, all slots are found to reflect the X-ray beam even when the bending radius was 4 m.

In theory, the X-rays from the bending source at SPring-8 can be focused to 0.2 mm but, in this case, the width of the focused beam is limited by the polygonal nature of the bent crystal. The horizontal size of the focused beam was narrowed down to a size corresponding to that of one crystal segment. Since beams from 17 segments overlap at the focal spot, the flux density would, ideally, be increased 17 times. Fig. 5 shows the spatial intensity profile measured at 40 keV by scanning

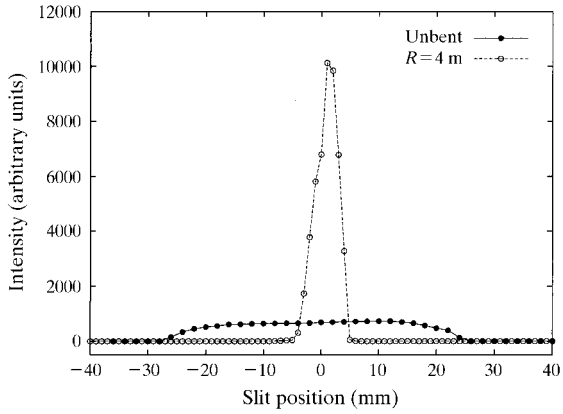

Figure 5
Horizontal scan through the focus with the second crystal.

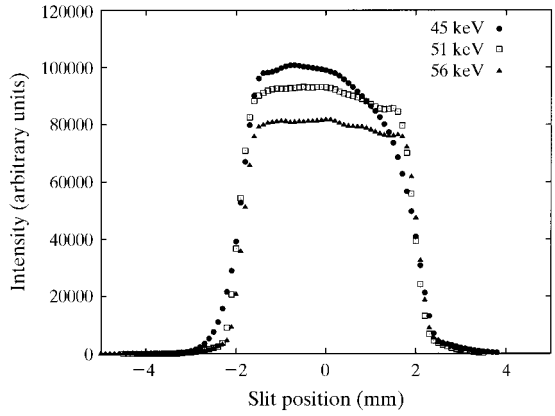

Figure 7
Horizontal beam profiles at energies from 45 keV to 56 keV.

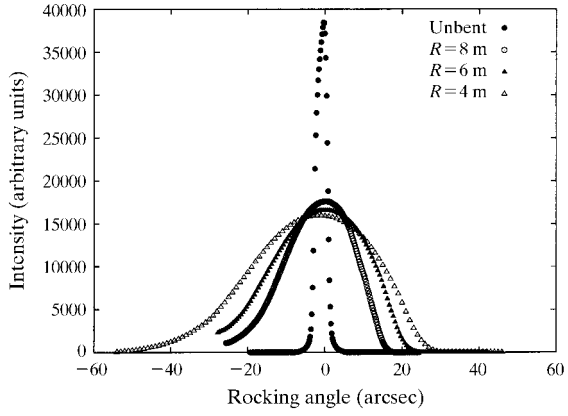

Figure 6
Rocking-curve profiles of the total flux while focusing at 40 keV.

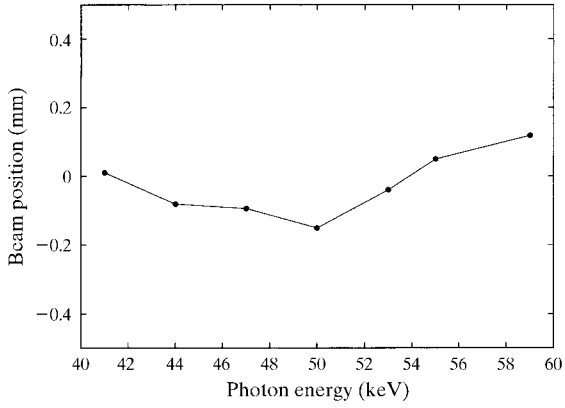

Figure 8
Beam height in the experimental hutch measured from 40 keV to 60 keV.

the slit horizontally at the 3:1 focus position for flat and bent (R = 4 m) crystals. The slit used was 0.5 mm wide and made of tungsten carbide. The measured increase of the flux density at the focal point was 15 times more than that of the flattened crystal, which is a little less than the ideal value (17 times) owing to the smaller diffraction efficiency of the bent crystal.

The rocking-curve profiles for the corresponding bending radius using full beam at 40 keV are shown in Fig. 6. The full width at half-maximum (FWHM) of the rocking curve at R = 8 m was wider than that when the crystal was flattened because of the cylindrical nature of the bent crystal. A part of this broadening may be caused by an undesirable twist of the crystal, but Fig. 5 indicates that loss of intensity should be small. The FWHM at R = 4 m looks slightly wider than that at R = 8 m. A slight and gradual decrease in the peak intensity was observed when R was changed from 8 m to 4 m. The tails of the profile when the X-ray beam is focused look rather symmetric. These symmetric profiles suggest that the sagittal-focusing crystal be bent almost ideally.

The spatial intensity profiles at different X-ray energies are shown in Fig. 7. These profiles at energies of 45, 51 and 56 keV were measured at a sample position of a diffractometer in the experimental hutch. Sharp-edged trapezoid profiles show the present crystal bent to ideal curvature at each energy value.

A dynamic sagittal-focusing (Lamble & Heald, 1992) test was performed between 40 keV (R = 4 m) and 60 keV (R = 2 m). The beam height at the sample position was measured after optimizing the bending radius and the parallelism between the first and second crystals. The deviation of the beam height in the energy range was within ±0.15 mm, as shown in Fig. 8. The preliminary set-up with flat–flat double crystals was carried out before installing the bender. The deviation of the beam height with flat–flat double crystals was 0.1 mm in the range from 40 keV to 60 keV. The practical deviation of the beam height with the bender was somewhat larger than expected. When the bending is performed, the fixed point is not the surface of the bent crystal but the center of the crystal. Because of the thickness and polygonal nature of the bent crystal, the practical beam height was changed from 40 keV to 60 keV. However, the beam deviation should be negligible in most experiments.

One of the problems to be solved is how to manage the so-called Compton heating (Kawata *et al.*, 1989) which causes instability as well as a decrease of the throughput owing to

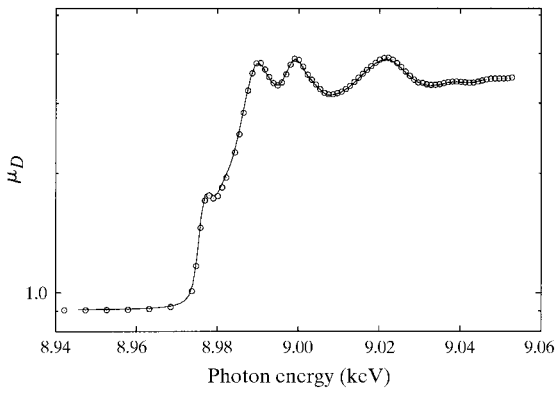

Figure 9
Near-edge absorption spectra of Cu foil, registered in a dynamical focusing mode (circles) and with a flat crystal (line). The energy resolution is not affected, as all edge structures are reproduced without distortion.

lattice-spacing mismatch between the first and second crystals. The heating effect becomes more serious for higher-energy X-rays. An efficient cooling system for both crystal and bending mechanism should be developed.

This sagittal-focus bender is designed for an inclined double-crystal monochromator. The properties of sagittal focusing with inclined geometry and an Si(111) reflection were tested. In Fig. 9 we compare a near-edge spectrum of a Cu foil registered in a dynamically focusing mode with a normal flat crystal. The two spectra are identical so we conclude that energy resolution is not affected by sagittal focusing, nor are any distortions introduced.

The dynamical sagittal focusing in the wide energy range from 8.5 keV to 60 keV without exchanging monochromatic crystals will become possible by using the present bending mechanism in the inclined geometry.

4. Summary

The sagittal focusing was tested by using a fixed-height exit bender that is designed for bending-magnet beamlines at SPring-8. The flux density of the focusing X-ray beam was increased by 15 times compared with that using flat–flat double crystals. The center of the focused beam position remained within 0.3 mm when the bending radius was optimized according to respective energy values. In this test, the storage-ring current was 70 mA and the output beam was stable during data collection. It is necessary, however, to solve the radiation problem, because the ring current of the SPring-8 storage ring will increase up to 100 mA. A water-cooled system should be required for both crystal and bending mechanism for protection against Compton heating.

References

Furukawa, Y. & Ishikawa, T. (1995). *SPring-8 Annual Report*, pp. 191–192. SPring-8, Kamigori-cho, Hyogo-ken 678-12, Japan.
Kawata, H., Miyahara, T., Yamamoto, S., Sioya, T., Kitamura, H., Sato, S., Asaoka, S., Kanaya, N., Iida, A., Mikuni, A., Sato, M., Iwazumi, T., Kitajima, Y. & Ando, M. (1989). *Rev. Sci. Instrum.* **66**, 1885–1888.
Koyama, A., Nomura, M., Kawata, H., Iwazumi, T., Sato, M. & Matsushita, T. (1991). *Rev. Sci. Instrum.* **63**, 916–919.
Kushnir, V. I., Quitana, J. P. & Geogopoulos, P. (1993). *Nucl. Instrum. Methods A*, **328**, 588–591.
Kushnir, V. I., Quitana, J. P. & Rosenbaum, G. (1995). *Nucl. Instrum. Methods A*, **362**, 592–594.
Lamble, G. M. & Heald, S. M. (1992). *Rev. Sci. Instrum.* **63**, 880–883.
Matsushita, T., Ishikawa, T. & Oyanagi, H. (1986). *Nucl. Instrum. Methods A*, **246**, 377–379.
Pascarelli, S., Boscherini, F., D'Acapito, F., Hrdy, J., Meneghini, C. & Mobilio, S. (1996). *J. Synchrotron Rad.* **3**, 147–155.
Sparks, C. J. Jr, Borie, B. S. & Hastings, J. B. (1980). *Nucl. Instrum. Methods*, **172**, 237–242.
Sparks, C. J. Jr, Borie, B. S. & Hastings, J. B. (1982). *Nucl. Instrum. Methods*, **195**, 73–78.
Uruga, T., Kimura, H., Kohmura, Y., Kuroda, M., Nagasawa, H., Ohtomo, K., Yamaoka, H., Ishikawa, T., Ueki, T., Iwasaki, H., Hashimoto, S. & Kashihara, Y. (1995). *Rev. Sci. Instrum.* **66**, 2254–2256.
Yabashi, M., Yamazaki, H., Tamasaku, K., Goto, S., Takeshita, K., Mochizuki, T., Yoneda, Y., Furukawa, Y. & Ishikawa, T. (1999). *Proc. SPIE*, **3773**, 2–13.

Received 5 May 2000 • Accepted 17 October 2000